The Meteoritical Society

Meteoritics & Planetary Science 51, Nr 11, 2061–2072 (2016)
doi: 10.1111/maps.12576

Postcrystallization metasomatism in shergottites: Evidence from the paired meteorites LAR 06319 and LAR 12011

Geoffrey H. HOWARTH[1,2*], Yang LIU[3,4], Yang CHEN[3,4], John F. PERNET-FISHER[1], and Lawrence A. TAYLOR[1]

[1]Earth and Planetary Sciences Department, Planetary Geosciences Institute, University of Tennessee, Knoxville, Tennessee 37996, USA
[2]Department of Geological Sciences, University of Cape Town, Rondebosch 7701, South Africa
[3]Jet Propulsion Laboratory, California Institute of Technology, Pasadena, California 91109, USA
[4]Division of Geology and Planetary Science, California Institute of Technology, Pasadena, California 91125, USA
[*]Corresponding author. E-mail: ghhowarth@gmail.com

(Received 22 June 2015; revision accepted 12 October 2015)

Abstract–Apatite is the major volatile-bearing phase in Martian meteorites, containing structurally bound fluorine, chlorine, and hydroxyl ions. In apatite, F is more compatible than Cl, which in turn is more compatible than OH. During degassing, Cl strongly partitions into the exsolved phase, whereas F remains in the melt. For these reasons, the volatile concentrations within apatite are predictable during magmatic differentiation and degassing. Here, we present compositional data for apatite and merrillite in the paired enriched, olivine-phyric shergottites LAR 12011 and LAR 06319. In addition, we calculate the relative volatile fugacities of the parental melts at the time of apatite formation. The apatites are dominantly OH-rich (calculated by stoichiometry) with variable yet high Cl contents. Although several other studies have found evidence for degassing in the late-stage mineral assemblage of LAR 06319, the apatite evolutionary trends cannot be reconciled with this interpretation. The variable Cl contents and high OH contents measured in apatites are not consistent with fractionation either. Volatile fugacity calculations indicate that water and fluorine activities remain relatively constant, whereas there is a large variation in the chlorine activity. The Martian crust is Cl-rich indicating that changes in Cl contents in the apatites may be related to an external crustal source. We suggest that the high and variable Cl contents and high OH contents of the apatite are the results of postcrystallization interaction with Cl-rich, and possibly water-rich, crustal fluids circulating in the Martian crust.

INTRODUCTION

Martian meteorites represent our only source of material from the surface of Mars, and are fundamental in our understanding of the evolution of the planet. These meteorites are broadly divided into several groups, all of which are igneous rock types (1) chassignites, (2) nakhlites, and (3) shergottites. Several exceptions are noted, such as Martian breccia meteorites (e.g., NWA 7034 and its pairs), as well as the orthopyroxenite (ALH 84001). The most abundant of these groups are the shergottites, which can be further subdivided into three groups: lherzolitic (poikilitic), olivine-phyric, and basaltic (diabasic). Furthermore, the shergottite meteorites can be broadly divided into three chemical subgroups, primarily based on the concentrations of rare earth elements (REE): "enriched, more oxidized" and "depleted, reduced" subgroups as well as a group intermediate but distinct between the enriched and depleted endmembers (e.g., Herd et al. 2002; Borg and Draper 2003). These subgroups have been interpreted to reflect formation from three separate geochemical reservoirs on Mars (e.g., Symes et al. 2008).

Apatite is a common late-stage interstitial mineral within shergottite meteorites, and is the dominant

volatile-bearing phase; apatite is significantly more abundant in the enriched shergottites. The relative volatile composition of apatite is important in understanding the volatile evolution of Martian magmas and the enriched shergottites represent the best samples available to study apatite. The partitioning of the volatile components between apatite and basaltic melt is unlike typical incompatible trace element partitioning, and is more similar to the partitioning of Mg-Fe between olivine and melt (e.g., Boyce et al. 2014; Doherty et al. 2014; McCubbin et al. 2015). Fluorine is more compatible than chlorine, which in turn is more compatible than hydroxyl. Therefore, during closed system apatite fractionation the volatile components of apatite will initially be F-rich, evolving toward Cl-rich compositions, and finally toward OH-rich compositions. In terrestrial mafic intrusions, cumulus apatite is F-rich consistent with the partition coefficients; however, later interstitial apatites may be either OH-F-rich or Cl-rich (e.g., Boudreau et al. 1986; Boudreau 1999; Willmore et al. 2000). Interstitial apatites that are OH-F-rich are interpreted to form after the exsolution/degassing of a hydrous Cl-bearing fluid phase. Chlorine strongly partitions into the fluid phase and is lost from the evolving magma, whereas fluorine remains in the melt (e.g., Mathez and Webster 2005; Aiuppa et al. 2009; Doherty et al. 2014). It must be noted that degassing not only results in the loss of chlorine, but also a substantial amount of water, and the evolution toward F-rich compositions during degassing is the result of simultaneous loss of Cl and water (e.g., Webster et al. 1999; Ustunisik et al. 2015). Chlorine-rich apatites in terrestrial mafic intrusions are generally interpreted to reflect equilibration with exsolved Cl-rich brines that migrate upward through the cumulate sequence from lower degassed cumulates (e.g., Boudreau and Kruger 1990; Boudreau 1999). Therefore, the volatile components of apatites may reflect either fractionation, which results in progressively increasing Cl and OH components, or degassing, which results in progressively decreasing Cl and OH components, or both. In addition, it has recently been shown that apatite in shergottite meteorites record evidence for the interaction of magmas with Cl-rich crustal fluids (e.g., Sharp et al. 2014; Williams et al. 2015; McCubbin et al. Forthcoming). In this case, the volatile components recorded by apatite would show trends inconsistent with degassing and more similar to a trend of fractionation with increased Cl.

In order to further investigate the volatile contents of Martian magmas, we present here compositional data for apatite and merrillite in the paired enriched, olivine-phyric shergottites LAR 12011 and LAR 06319. These meteorites represent one of two suites of paired meteorites belonging to this grouping of shergottites, the other being NWA 1068 and paired meteorites NWA 1110/1183/1775/2373/2969 (e.g., Barrat et al. 2002; Herd 2006; Filiberto et al. 2010). Previous studies on LAR 06319 have shown that the apatites are generally OH-rich (e.g., Balta et al. 2013), and late-stage degassing has been suggested to have affected residual liquids resulting in increased fO_2 conditions from early to late-stage phases (e.g., Basu Sarbadhikari et al. 2009; Peslier et al. 2010; Balta et al. 2013). Therefore, the main objective of this study is to understand the evolution and fractionation of fluorine, chlorine, and water in the late-stage residual liquids of the parent magmas for enriched, olivine-phyric shergottites, and to compare this with other Martian magmas. Specifically, we aim to address whether the changes in apatite volatile concentrations reflect degassing, fractionation, or assimilation of a Cl-rich crustal component.

ANALYTICAL TECHNIQUE

Fluorine and chlorine are moderately volatile elements, and analyzing these elements using an electron microprobe requires care (e.g., Stormer et al. 1993). The apatites in this study have been analyzed at a variety of conditions over the course of the study to determine the relative variability in analyzed concentrations at different analytical protocols. The apatites were analyzed using a CAMECA SX-100 EMP housed at the University of Tennessee. Two separate analytical protocols were used. First, the protocol recently outlined by Goldoff et al. (2012) was used as they have shown that the most accurate F and Cl concentrations are obtained using this method. Other recent studies on Martian meteorites have also adopted this methodology (e.g., Gross et al. 2013). They showed that the best results were obtained using an acceleration voltage of 10 kV with a 4 nA beam current for F, Cl, and Na first, followed by analysis of P, Si, Fe, Mg, Mn, and Ca at 15 kV and a 20 nA beam current. All these analyses were conducted with a defocused 10 μm beam, with peak and background counting times of 30 s and 15 s, respectively. Secondly, apatites were analyzed at more standard operating protocols using an accelerating voltage of 15 kV with 10 nA beam current for all elements. Similar to protocol 1, all analyses were conducted with a defocused 10 μm beam, with peak and background counting times of 30 s and 15 s, respectively. The standards used were from a block purchased from C.M. Taylor Corp. in 1988. Phosphorous, Ca, and F were calibrated on a fluoroapatite (Wilberforce apatite); Na on albite (Amelia Albite); Cl on HgCl; Mg on olivine #1; Si on diopside #5a; Fe on hematite; and Mn on spessartine

#4a. Data sets collected using both protocols are presented in Fig. 3. The dataset from Balta et al. (2013), used for comparison during the discussion section, was analyzed under operating conditions similar to that described in protocol 2.

RESULTS

Phosphate Composition

Apatites occur as discrete grains and complex apatite-merrillite intergrowths, as a late-stage interstitial groundmass phase. Merrillite is clearly distinguished in X-ray compositional maps by higher P_2O_5, Na_2O, and MgO; lower CaO; and the absence of a volatile component (Figs. 1 and 2). Merrillites are relatively homogeneous in composition with little variation within and between grains. Apatites within LAR 12011 are observed up to 200 μm in length, whereas those within LAR 06319 are generally <100 μm. It is generally difficult to discern the timing of merrillite versus apatite crystallization. Lath-shaped phosphates are observed split in half down the center giving no textural evidence for their relative timing of crystallization (Figs. 2a–c). Alternatively, more complex intergrowths observed as irregular shaped crystals give ambiguous evidence for the relative timing of apatite versus merrillite formation (Figs. 2d–f).

Apatites in LAR 12011 and LAR 06319 overlap in compositions, although several outliers in both samples are observed (Fig. 3). In both cases, the apatites are generally OH-rich relative to other Martian apatites, with a X-site occupancy of $F_{10–30}Cl_{8–30}OH_{50–70}$ (OH calculated by stoichiometry) (Table 1). The volatile contents of single apatite grains are generally constant and within the overall volatile distribution of apatites measured. However, several exceptions are noted; for example, apatite grain 5 in LAR 12011 is a complex irregular apatite-merrillite intergrowth with a distinct high-chlorine portion ($F_9Cl_{53}OH_{38}$) (Figs. 2d–f). Furthermore, apatite grain 1 in LAR 12011 is a coarse apatite lath where Cl-content varies from one end to the other (Figs. 2g and 2h). Balta et al. (2013) also noted Cl-rich apatite suggesting two separate apatite populations exist in LAR 06319.

The volatile ratios of the apatites show distinct trends. A positive trend is observed for F/Cl versus OH/Cl (Fig. 4a). In contrast, a negative trend is observed for F/Cl versus OH/F, characterized by decreasing OH/F with concurrent increase in F/Cl (Fig. 4b). The ratios of OH/Cl versus OH/F show a strong decrease in OH/Cl at initially constant OH/F, followed by a sharp increase in OH/F at low OH/Cl ratios (Fig. 4c).

Relative Volatile Fugacities

Recently, Patiño Douce and Roden (2006) developed a thermodynamic formulation for the calculation of relative volatile (F_2, Cl_2, H_2O) fugacities in melts that are in equilibrium with the apatite-merrillite pairs. Using this formalization, Gross et al. (2013) showed that the olivine-phyric shergottite NWA 6234 had volatile fugacities similar to that of terrestrial basalts and concluded that the volatile ratios were similar to that of MORB mantle. Furthermore, the relative volatile fugacities normalized using F, can be used to interpret degassing versus apatite fractionation trends (e.g., Gross et al. 2013; Howarth et al. 2015).

The relative volatile fugacities for LAR 06319 and LAR 12011 were calculated using the methods of Patiño Douce and Roden (2006), in order to assess and compare the relative volatile contents and their evolution, with other Martian meteorites and terrestrial magmas. The relative fluorine ($\Delta\log f(F_2)_{QFM}$), chlorine ($\Delta\log f(Cl_2)_{QFM}$), and water ($\Delta\log f(H_2O)_{QFM}$) fugacities are calculated using equations 1–3 based on endmember apatite-merrillite equilibria, and presented in Fig. 5. These equations are defined at the same pressure and temperature, and a fO_2 value of that calculated for LAR 06319 in previous studies (QFM−1.7; Basu Sarbadhikari et al. 2009). It must be emphasized that these equations do not calculate the absolute volatile fugacities, but rather the volatile fugacity ratios, allowing for the relative activity of F_2, Cl_2, and H_2O to be assessed. The $\log K$ term in equations 1–3 is the equilibrium constant defined by the endmember apatite-merrillite equilibria:

$$K = \{a[Ca_3(PO_4)_2]mer\}^3/\{a[Ca_5(PO_4)_3(F,Cl,OH)]ap\}^2$$

For detailed discussion on the derivation of equations 1–5 see the original work of Patiño Douce and Roden (2006). Detailed calculations using the formulas are given in the Data S1.

$$\Delta\log f(F_2)_{QFM} = 0.5\Delta\log fO_2 - \log K_{F-phosphates} \quad (1)$$

$$\Delta\log f(Cl_2)_{QFM} = 0.5\Delta\log fO_2 - \log K_{Cl-phosphates} \quad (2)$$

$$\Delta\log f(H_2O)_{QFM} = -\log K_{OH-phosphates} \quad (3)$$

The $\Delta\log f(F_2)_{QFM}$ and $\Delta\log f(Cl_2)_{QFM}$ are within the previously reported Martian ranges. However, the

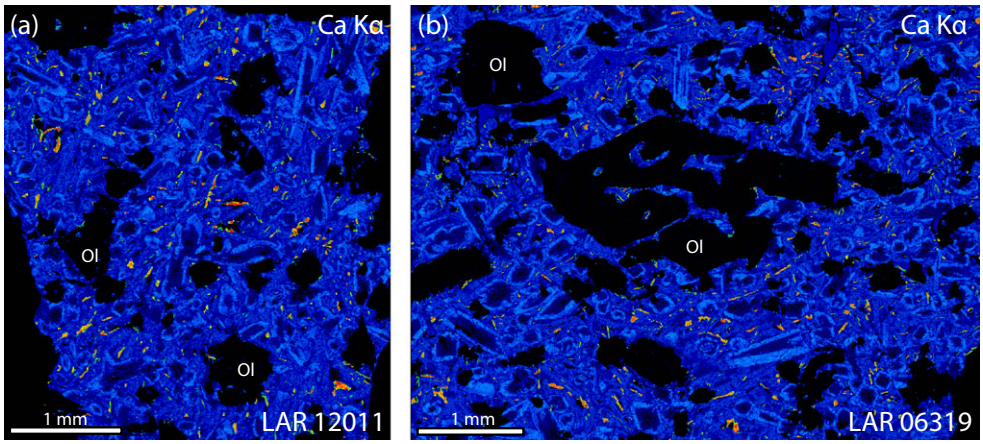

Fig. 1. Calcium Kα compositional maps for sections of (a) LAR 12011 and (b) LAR 06319, 37. Phosphates are the red/orange (brightest phase); the red colored phase represents slightly higher CaO content equivalent to apatite, whereas the orange color represents the merrillite. Olivine has no Ca and is observed as the dark phases. Pyroxenes are observed as zoned crystals from low-Ca (darker) cores to high-Ca (brighter) rims.

$\Delta\log f(H_2O)_{QFM}$ is significantly higher, which is consistent with the higher calculated OH component of the apatites. Furthermore, normalizing the $\Delta\log f(Cl_2)_{QFM}$ and $\Delta\log f(H_2O)_{QFM}$, using fluorine (equations 4–5), allows for further comparisons to be made.

$$\Delta\log f(Cl_2)F_2 = \Delta\log f(Cl_2)_{QFM} - \Delta\log f(F_2)_{QFM} \quad (4)$$

$$\Delta\log f(H_2O)F_2 = \Delta\log f(H_2O)_{QFM} - \Delta\log f(F_2)_{QFM} \quad (5)$$

The $\Delta\log f(Cl_2)F_2$ and $\Delta\log f(H_2O)F_2$ for LAR 12011 and LAR 06319 overlap as expected, and overlap with previously calculated ranges for the Shergotty and QUE 94201 Martian meteorites, but are significantly different from the olivine-phyric shergottite NWA 6234 (Fig. 5a). The overall trend is similar to that of the trend interpreted to reflect apatite fractionation by Gross et al. (2013), although with a slightly steeper slope. However, degassing would be expected to result in lowering both the $\Delta\log f(Cl_2)F_2$ and $\Delta\log f(H_2O)F_2$ producing a similar trend to apatite fractionation but in the opposite direction (Fig. 6).

DISCUSSION

Controls on Late-Stage Volatile Evolution

Here, we evaluate three common processes that control the late-stage evolution of volatiles in basaltic magmas (1) fractionation, (2) degassing, and (3) assimilation/interaction with crustal components. In addition, it was recently shown that apatite volatile concentrations can be significantly affected, increasing the Cl contents, by shock process during ejection from Mars (Howarth et al. 2015). These authors showed that high Cl contents are associated with shock melts invading apatite grains in the lherzolitic shergottite NWA 7755; however, in the case of LAR 06319 and LAR 12011 no such textural observation has been made, suggesting that volatile redistribution during shock is unlikely a contributing factor.

Apatite Fractionation

Apatite is the major volatile-bearing phase in shergottite meteorites; therefore (in the absence of degassing), only if apatite is part of the fractionating assemblage will the F:Cl:OH ratio in the evolving melt change during crystallization. McCubbin et al. (Forthcoming) modeled the evolution of apatite compositions during closed system fractionation of a Martian magma showing that the initial apatites to crystallize are F-rich evolving toward the OH-Cl binary. As the apatite compositions approach the OH-Cl binary there is a sharp rise in the Cl contents that is the result of Cl becoming more compatible than OH in apatite crystallizing from a melt with low F contents; once the OH-Cl binary is intersected the apatites evolve toward the hydroxyapatite endmember (Fig. 3b) (McCubbin et al. Forthcoming).

This fractionation trend is not consistent with that observed for apatites in the LAR 06319 and LAR 12011 shergottites, where the overall trend is controlled by the large variation in the Cl contents (Fig. 3). The relative volatile fugacities plotted as ratios with F in Fig. 6 are

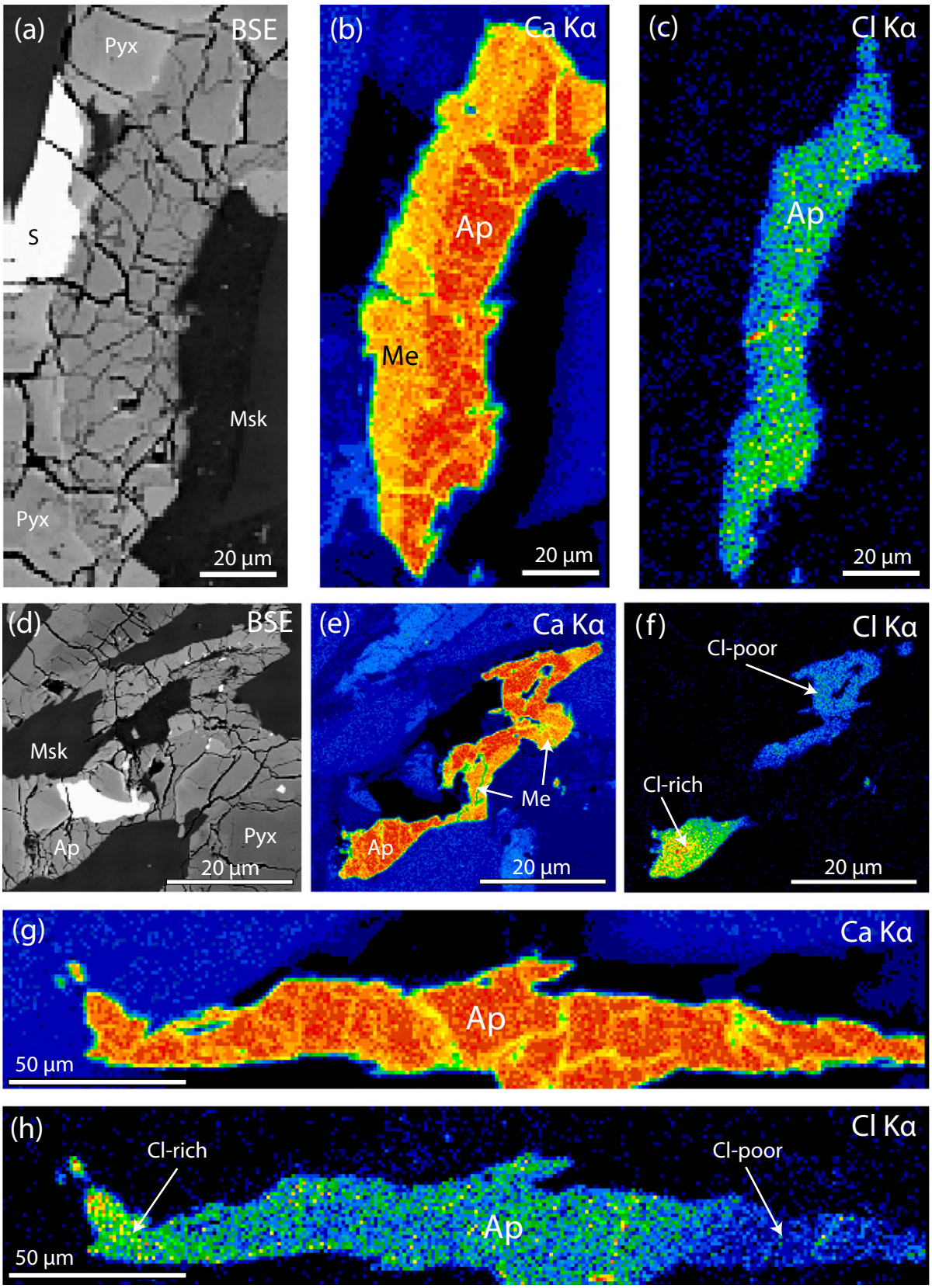

Fig. 2. Backscatter electron images (BSE) and X-ray compositional maps for apatites from the enriched, olivine-phyric shergottite LAR 12011. Ap = apatite, Me = merrillite, Pyx = pyroxene, Msk = maskelynite, S = sulfide.

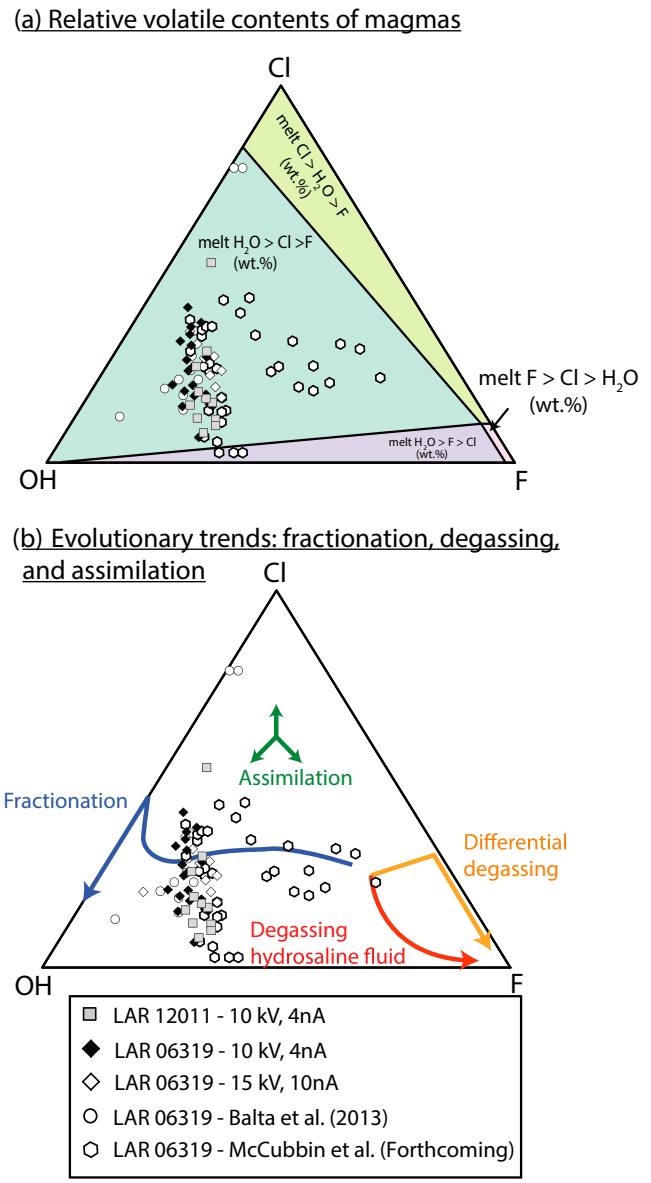

Fig. 3. Ternary plot of apatite X-site occupancy (mole%) for LAR 12011 and LAR 06319. Data from this study are plotted with those presented by Balta et al. (2013) and McCubbin et al. (Forthcoming). a) Apatite data plotted with fields for relative parental volatile contents after McCubbin et al. (2013). b) Apatite data plotted with the evolutionary trends for apatite during fractionation, degassing, and assimilation after McCubbin et al. (Forthcoming).

similar to that of the apatite fractionation trend, whereas Fig. 5 suggests that fractionation is unlikely the controlling mechanism in this case. The (Δlog $f(F_2)_{QFM}$) and (Δlog $f(H_2O)_{QFM}$) show little variation (Fig. 5b), indicating their activities remain stable. In contrast, (Δlog $f(Cl_2)_{QFM}$) shows a large range (Figs. 5a and 5c), indicating some other process is controlling the volatile activities.

Volatile Degassing

Generally, juvenile volatile (primary magmatic volatile) degassing during magma evolution results in the loss of water and Cl, and retention of F in the melt (e.g., Ustunisik et al. 2011, 2015). If degassing occurs during apatite crystallization, the apatites evolve toward F-rich compositions. Furthermore, degassing strongly decreases the water to halogen ratios in basaltic melts as well as increasing the F/Cl ratio (e.g., Webster et al. 1999). Degassing can occur in two separate processes that are characterized by different apatite evolutionary paths. (1) Differential degassing at low pressure and low fO_2 (<QFM−4) where H_2 is preferentially lost over H_2O and Cl, resulting in the evolution of apatite composition toward the F-Cl binary at constant F/Cl ratio followed by later evolution to fluoroapatite (e.g., Ustunisik et al. 2011, 2015) (Fig. 3b). (2) Hydrosaline fluid degassing/exsolution at higher pressures and higher fO_2 conditions (~QFM), in which Cl and H_2O partition into an exsolving hydrosaline fluid (brine), and F is retained in the melt (e.g., Carroll and Webster 1994; Webster et al. 1999) (Fig. 3b). This is observed in terrestrial intrusions where apatites formed after hydrosaline fluid formation are OH-F-rich (e.g., Boudreau et al. 1986; Willmore et al. 2000); similar trends are observed for cumulus Martian rocks (e.g., Howarth et al. 2015).

The apatites analyzed in LAR 12011 and LAR 06319 are not consistent with differential degassing at low pressures, as described above (Fig. 3). Two separate trends are observed: Firstly, the data presented in this study, along with that of Balta et al. (2013) and some of the data from McCubbin et al. (Forthcoming), show a trend from Cl-rich compositions trending steeply toward the OH-F binary (Fig. 3). A second trend is observed in some of the data presented by McCubbin et al. (Forthcoming), starting from similarly Cl-rich compositions, but trending toward the F apex (Fig. 3). The former trend is not consistent with typical degassing of a basaltic magma, whereas the latter trend is similar to that of degassing, but with significantly higher Cl starting compositions. A strong positive correlation is observed between F/Cl and OH/Cl for apatite observed in this study (trend 1) (Fig. 4b), suggesting decoupling of the water to halogen ratios with regards to F/Cl, again not consistent with degassing in typical basaltic magmas.

Evidence for late-stage degassing of the LAR 06319 meteorite has been presented by several authors. Balta et al. (2013) described Fe^{3+}-rich oxides in association with sulfides in the interstitial groundmass, which they interpreted to result from a reaction between Fe in the sulfide and O in the melt due to decreasing sulfur activity during S-degassing. Degassing of a hydrous phase has been linked with increasing oxygen fugacity in residual melts (e.g., Mathez 1984; Bell and Simon 2011). Indeed,

Table 1. Representative microprobe analyses for apatites from LAR 06319 and LAR 12011.

	LAR06319 – 4 nA			LAR12011 – 4 nA			LAR06319 – 10na		
	Ap1_1	Ap4_1	Ap8_2	Ap1_1	Ap2_1	Ap3_1	Ap1	Ap3	Ap2
P_2O_5	41.1	41.5	40.7	41.4	41.39	41.8	41.37	41.29	41.59
SiO_2	0.14	0.37	0.58	0.22	0.54	0.13	0.29	1.14	0.37
MgO	0.04	0.05	0.06	0.09	0.06	0.06	0.62	0.07	0.01
CaO	54.9	54.3	53.9	54.6	54.8	54.5	52.6	53.5	55.6
MnO	0.14	0.12	0.08	0.12	0.09	0.09	n.a	n.a	n.a.
FeO	0.63	0.84	0.72	0.97	0.67	0.69	1.43	0.72	0.71
Na_2O	0.09	0.05	0.04	0.10	0.09	0.06	0.46	0.12	0.04
F	0.74	0.78	0.61	0.72	1.13	1.02	0.43	0.49	1.07
Cl	1.90	1.41	1.40	2.02	0.79	1.10	1.38	2.38	1.19
O=F, Cl	0.74	0.64	0.57	0.76	0.65	0.68	0.49	0.74	0.72
Total	100.45	100.07	98.74	101.00	100.15	100.14	99.12	100.47	101.26
Normalized to 8 cations									
P	2.99	2.97	2.95	2.98	2.95	2.99	2.98	2.91	2.97
Si	0.01	0.03	0.05	0.02	0.05	0.01	0.02	0.09	0.03
Mg	0.01	0.01	0.01	0.01	0.01	0.01	0.08	0.01	0.00
Ca	4.93	4.92	4.93	4.90	4.92	4.93	4.75	4.92	4.94
Mn	0.01	0.01	0.01	0.01	0.01	0.01	n.a.	n.a.	n.a.
Fe	0.04	0.06	0.05	0.07	0.05	0.05	0.10	0.05	0.05
Na	0.01	0.01	0.01	0.02	0.01	0.01	0.07	0.02	0.01
Total	8.00	8.00	8.00	8.00	8.00	8.00	8.00	8.00	8.00
OH	0.52	0.58	0.63	0.51	0.58	0.56	0.68	0.52	0.54
F	0.20	0.21	0.17	0.20	0.31	0.28	0.12	0.13	0.29
Cl	0.28	0.21	0.21	0.30	0.12	0.16	0.20	0.35	0.17

increases in oxygen fugacity during crystallization noted by Basu Sarbadhikari et al. (2009) and Peslier et al. (2010) are also linked with degassing and auto-oxidation at a late stage of magmatic evolution. However, degassing of a hydrous phase is not observed in the apatite compositional data presented in this study, as indicated by the OH-rich nature of the apatites. Therefore, although a subset of the data (trend 2) may indicate degassing from an original Cl-rich composition, the bulk of the data is not consistent with Cl-rich hydrous degassing from a single source.

Assimilation/Interaction with a Crustal Component

Open system processes such as assimilation of crustal material or interaction with crustal fluids can have a significant effect on the volatile budget of evolving magmas and consequently the apatite compositions. These processes can drive apatite compositions in any direction, depending on the composition of the assimilant (Fig. 3b). The Martian crust has been shown to be Cl-rich with abundant evidence for the circulation of Cl-rich fluids (e.g., Bridges et al. 2001; McCubbin et al. 2013; Filiberto et al. 2014). Therefore, interaction of Martian magmas with crustal components can significantly affect the Cl concentrations of the apatite. The decoupling of the water to halogen ratios and the high and variable Cl concentrations observed for the LAR 06319 and LAR 12011 meteorites can only be explained by open system behavior of the volatiles with additions of Cl to the apatite. These interpretations are also consistent with those of McCubbin et al. (Forthcoming) for several other Martian meteorites with high/variable Cl contents that indicate additions of crustal components. Therefore, regardless of whether degassing occurred, the high Cl concentrations indicate addition of Cl, and possibly water, at some stage during the evolution of the LAR 06319 and LAR 12011 shergottites. Furthermore, this suggests that the calculated relative volatile fugacities do not represent the volatile activities of the original parent magma and have been modified at some stage during evolution.

Timing of Chlorine (and Water) Addition

The exact timing of the chlorine addition responsible for Cl enrichment of the apatite is important in order to correctly interpret the primary volatile concentrations in apatites. Three potential scenarios exist that may explain the apatite evolutionary trends observed in the F-Cl-OH ternary (1) alteration by late-stage deuteric fluids; (2) assimilation of crustal material on emplacement of the parent magma into the crust prior to apatite crystallization; and (3) late-stage interaction of Cl-rich, and likely water-rich, crustal fluids with previously crystallized apatite.

1. *Deuteric fluids*. Chlorapatites are commonly observed in layered intrusions on Earth where they are

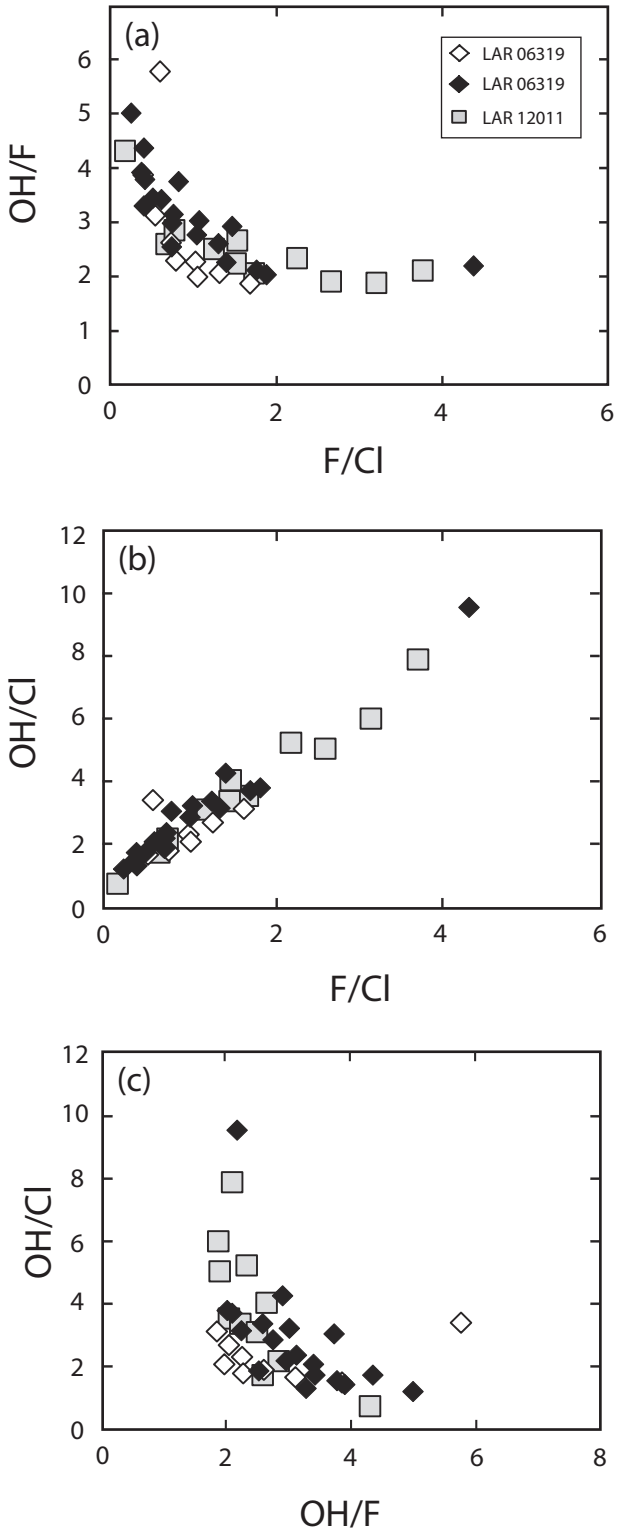

Fig. 4. Apatite volatile ratios for LAR 12011 and LAR 06319. The data for LAR 06319 represent the two different analytical protocols described in the Analytical Technique section. The filled diamonds represent the Protocol 1 after Goldoff et al. (2012) methods, whereas the open diamonds represent the standard EMP protocol 2.

interpreted to represent late-stage intercumulus phases that interacted with circulating Cl-rich brines exsolved from the evolving magma (e.g., Boudreau et al. 1986; Willmore et al. 2000). Howarth et al. (2015) reported apatite compositions in the NWA 7755 cumulate lherzolitic shergottite that indicate the formation and loss of such a Cl-rich brine. Although olivine megacrysts in the olivine-phyric shergottites are likely to have crystallized at depth in a staging chamber or *en route* to the surface (e.g., Balta et al. 2013), generally olivine-phyric shergottites are believed to represent shallow level intrusions or lavas extruding at the surface. Olivine megacrysts survive in the magmas due to the lack of fractionation; therefore, it is unlikely that the Cl-rich apatite composition in the LAR 06319 and LAR 12011 meteorites are related to Cl-rich brines exsolved from a cumulate pile.

2. *Crustal assimilation*. Apatite is a late-stage crystallizing phase; thus, thermally it would not be possible to assimilate crustal material and crystallize late-stage apatite at low temperatures simultaneously. In this case, assimilation must have occurred early, suggesting that the melt would have had a specific F-Cl-OH starting composition, which then evolved along either degassing or fractionation trends. As discussed above, neither degassing nor fractionation from a single starting composition (a single source) can explain the observed trend. The alternative would be degassing of an anhydrous Cl-rich fluid. Such degassing has been interpreted for lunar basalts based on very variable and heavy $\delta^{37}Cl$; however, the $\delta^{37}Cl$ for shergottites is significantly lower and does not indicate similar degassing to that observed on the Moon (e.g., Sharp et al. 2010).
3. *Circulating Cl-rich (possibly water-rich) crustal fluids*. Alternatively, Cl-rich fluids circulating in the Martian crust may have interacted with the basalt after crystallization of the apatite. In this case, the apatite compositions would simply show a large range in Cl (and OH) contents and volatile ratios depending on the degree to which they interacted with the fluid. The evidence of degassing presented by Balta et al. (2013) and Peslier et al. (2010) discussed above would have initially resulted in the evolution of apatite compositions to the F-rich apex, as expected through typical degassing trends. Subsequently, the F-rich apatite would have been overprinted by interaction with Cl-rich (possibly water-rich), F-poor crustal fluids resulting in scattered data points with variable enrichment in Cl and OH (Fig. 3). It is also likely that these fluids would interact with other phases such as oxides and sulfides, and indeed this may be the case. Balta et al. (2013) described, in LAR 06319, the presence of nearly pure iron-oxide grains and

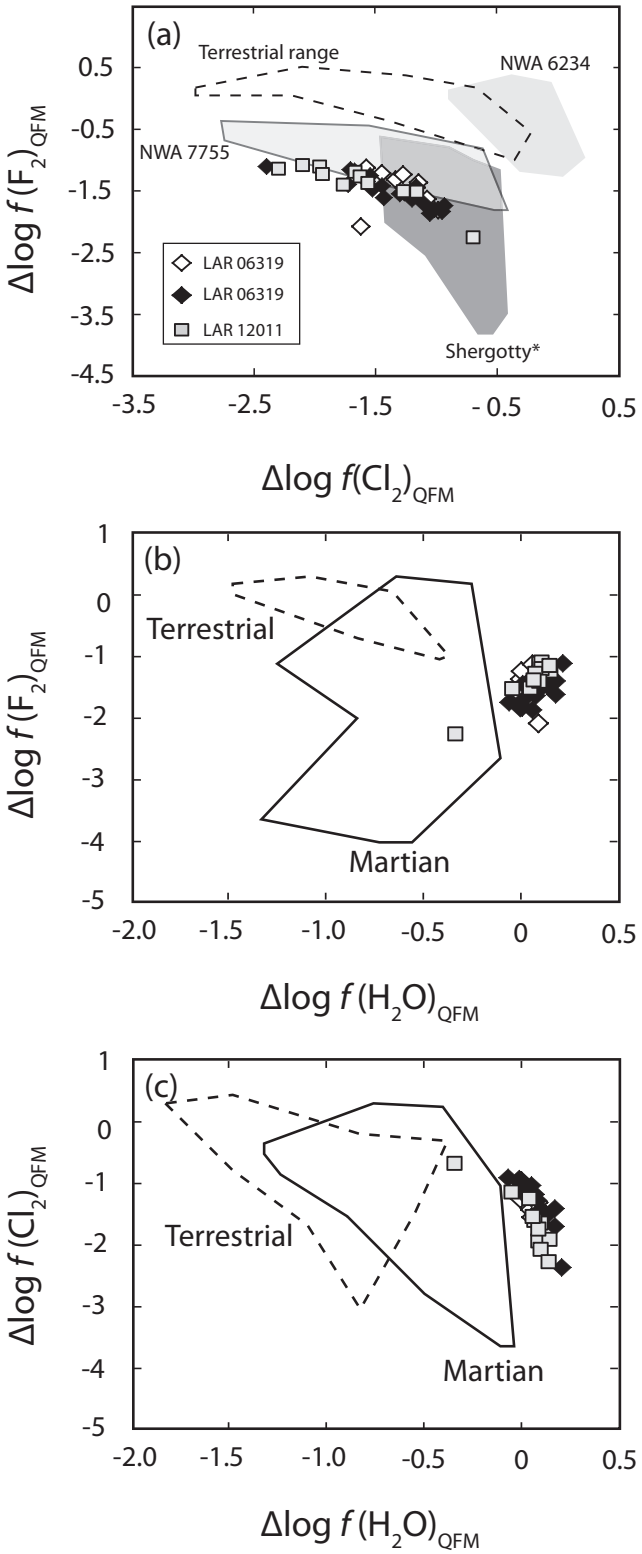

Fig. 5. Calculated relative volatile fugacities in melts using apatite-merrillite equilibria in the enriched, olivine-phyric shergottites LAR 12011 and LAR 06319. Volatile fugacities were calculated using the methods developed by Patiño Douce and Roden (2006). The field for terrestrial range is after Gross et al. (2013), along with the field for NWA 6234 and Shergotty. The field for NWA 7755 is after Howarth et al. (2015). The Martian field in (b) and (c) is a combined field for the above reference data, as they all overlap one another. The data for LAR 06319 represent the two different analytical protocols described in the Analytical Technique section. The filled diamonds represent the Protocol 1 after Goldoff et al. (2012) methods, whereas the open diamonds represent the standard EMP protocol 2.

associated sulfides, which they ascribed to sulfur degassing. Alternatively, this association of Fe^{3+}-rich oxides may be related to postcrystallization circulation of Cl-rich, oxidizing fluids, altering the oxides similarly to the apatites. Further detailed work is required to constrain such a mechanism.

The recent studies of Usui et al. (2012) and Hu et al. (2014) provide additional important constraints on the timing of crustal interaction. Usui et al. (2012) showed that olivine-hosted melt inclusions in LAR 06319 have D/H ratios indicative of a surface water reservoir. Although one may intuitively suggest that melt inclusions would have been shielded from later interactions with crustal fluids, Hu et al. (2014) showed that this is incorrect. These authors showed that the D/H values are well zoned within melt inclusions in the GRV 020090 shergottite with significantly higher values at the margins. They interpreted this feature to result from late-stage, postcrystallization percolation of a water-rich fluid circulating within the Martian crust. Further evidence for subsurface water activity on Mars was presented by Chen et al. (2015) who found high D/H ratios in impact melt glasses. They interpreted these ratios to indicate mixing of two volatile sources, a magmatic source and aqueous alteration source, providing additional evidence for the percolation of aqueous fluids in the Martian crust. Therefore, the high OH and Cl contents of apatite analyzed in this study, along with the high D/H value for melt inclusions analyzed by Usui et al. (2012) is consistent with late-stage, postcrystallization interaction with circulating crustal fluids that were both Cl-rich and water-rich.

However, further ambiguous evidence is observed in the $\delta^{37}Cl$ data presented in the literature for LAR 06319 apatite. Recently, it has been suggested that the $\delta^{37}Cl$ isotopic composition of the Martian mantle (<−2‰) and crust (>0‰) are different, and that apatites in Martian meteorites show a broad range from mantle (e.g., RBT 04262) to mantle-crust mixtures (e.g., Los Angeles) to more crustal compositions (NWA 7034) (e.g., Sharp et al. 2014; Shearer et al. 2014; Williams et al. 2015). Specifically, apatite in LAR 06319 has low $\delta^{37}Cl$ (−2 to −4‰; Sharp et al. 2011), suggesting that the apatites crystallized from mantle derived melts with little to no interaction with a crustal component. The Cl

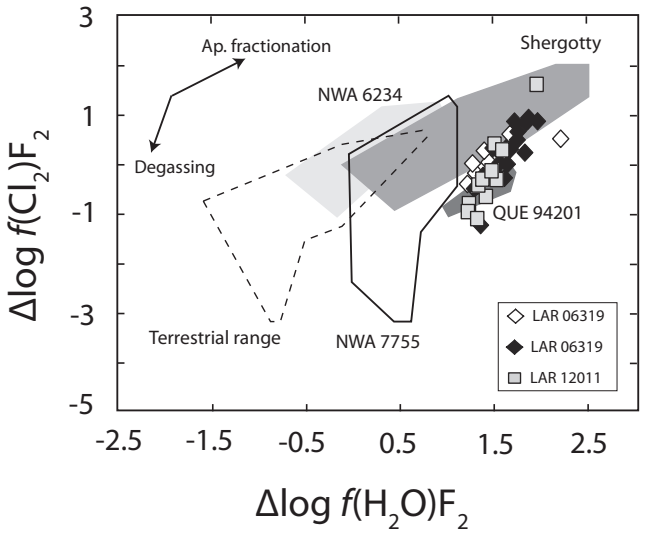

Fig. 6. Chlorine and water fugacities in melts normalized using fluorine for apatite in LAR 12011 and LAR 06319, and comparison with values calculated for other Martian meteorites and terrestrial apatites reported by Gross et al. (2013) and Howarth et al. (2015). The data for LAR 06319 represent the two different analytical protocols described in the Analytical Technique section. The filled diamonds represent the Protocol 1 after Goldoff et al. (2012) methods, whereas the open diamonds represent the standard EMP protocol 2.

concentrations reported for apatite in LAR 06319 by Sharp et al. (2011) were ~0.7 wt.%, which is on the lower end of compositions reported here. Furthermore, McCubbin et al. (Forthcoming) suggested that apatite compositions in lherzolitic shergottite RBT 04261 also indicate assimilation of a crustal component. However, similarly to LAR 06319 the δ^{37}Cl for RBT 04261 is low (~−3‰), interpreted as representing pristine mantle (Shearer et al. 2014). If indeed our interpretation is correct, suggesting that Cl- and OH-rich rich apatite is recording interaction with a crustal fluid, an important question arises: "what is the source of this Cl-rich component and why does it not have a heavy δ^{37}Cl isotopic signature as expected for a crustal reservoir." These questions cannot be answered in this contribution, and require additional detailed analysis of the LAR 06319 and LAR 12011 apatites so as to incorporate the full range of Cl concentrations observed. However, the high and variable Cl and OH contents of the apatite and the D/H ratios reported by Usui et al. (2012) can only be reconciled with a crustal input of Cl and water.

SUMMARY

Apatite compositions in the LAR 06319 and LAR 12011 paired shergottites are both OH- and Cl-rich, and are generally inconsistent with both fractionation and degassing trends. The enrichment in both OH and Cl is linked to a late-stage overprinting by circulating fluids in the Martian crust, postcrystallization. This interpretation is consistent with recent studies of D/H ratios in melt inclusions and shock melts in shergottites (Usui et al. 2012; Hu et al. 2014; Chen et al. 2015) as well as data for several other shergottites (McCubbin et al. Forthcoming). However, this interpretation is not consistent with the current interpretations for the δ^{37}Cl isotopic variation in shergottites.

The evolution of the volatile concentrations of the apatites in the LAR 06319 and LAR 12011 can be summarized in several steps: Initial crystallization as part of the late-stage mineral assemblage, with concurrent degassing of the magma leading to an evolutionary trend toward the F-rich apex of the apatite ternary. This trend was then overprinted during step 2: postcrystallization percolation of OH- and Cl-rich crustal fluids, which produced variably Cl-enriched apatites with relatively constant yet high OH content.

Therefore, apatite volatile concentrations in shergottite meteorites can be affected by a variety of pre- (degassing), syn- (fractionation), and post- (interaction with crustal fluids) crystallization mechanisms. These processes need to be carefully evaluated prior to interpretation on the volatile compositions of parental magmas, and indeed their mantle source. Furthermore, interpretation of a crustal source for enriched OH and Cl in the apatite suggests that the fractionation of Cl isotopes between crust and mantle needs to be carefully evaluated with apatite evolutionary trends to provide robust constraints on mantle versus crustal δ^{37}Cl compositions.

Acknowledgments—This work was supported by NASA Cosmochemistry grant NNX11AG58G, awarded to LAT. We thank Allen Patchen for assistance with electron microprobe analyses. YL acknowledge the partial support by NASA Cosmochemistry grants NNN13D465T, and support from the Jet Propulsion Laboratory, which is managed by the California Institute of Technology under the contract with NASA. We are extremely grateful to Francis McCubbin and Justin Filiberto for detailed and thorough reviews, which greatly aided the overall content and discussion of this manuscript. We also thank Cyrena Goodrich for editorial handling.

Editorial Handling—Dr. Cyrena Goodrich

REFERENCES

Aiuppa A., Baker D. R., and Webster J. D. 2009. Halogens in volcanic systems. *Chemical Geology* 263:1–18.

Balta J. B., Sanborn M., McSween H. Y., and Wadhwa M. 2013. Magmatic history and parental melt composition of olivine-phyric shergottite LAR 06319: Importance of

magmatic degassing and olivine antecrysts in Martian magmatism. *Meteoritics & Planetary Science* 48:1359–1382.

Barrat J. A., Jambon A., Bohn M., Gillet P., Sautter V., Göpel C., Lesourd M., and Keller F. 2002. Petrology and chemistry of the picritic shergottite Northwest Africa 1068 (NWA 1068). *Geochimica et Cosmochimica Acta* 66:3505–3518.

Basu Sarbadhikari A., Day J. M., Liu Y., Rumble D., and Taylor L. A. 2009. Petrogenesis of olivine-phyric shergottite Larkman Nunatak 06319: Implications for enriched components in Martian basalts. *Geochimica et Cosmochimica Acta* 73:2190–2214.

Bell A. S. and Simon A. 2011. Experimental evidence for the alteration of the Fe3 + /ΣFe of silicate melt caused by the degassing of chlorine-bearing aqueous volatiles. *Geology* 39:499–502.

Borg L. E. and Draper D. S. 2003. A petrogenetic model for the origin and compositional variation of the Martian basaltic meteorites. *Meteoritics & Planetary Science* 38:1713–1731.

Boudreau A. 1999. Fluid fluxing of cumulates: The JM reef and associated rocks of the Stillwater Complex, Montana. *Journal of Petrology* 40:755–772.

Boudreau A. E. and Kruger F. J. 1990. Variation in the composition of apatite through the Merensky cyclic unit in the western Bushveld Complex. *Economic Geology* 85:737–745.

Boudreau A. E., Mathez E. A., and McCallum I. S. 1986. Halogen geochemistry of the Stillwater and Bushveld Complexes: Evidence for transport of the platinum-group elements by Cl-rich fluids. *Journal of Petrology* 27:967–986.

Boyce J. W., Tomlinson S. M., McCubbin F. M., Greenwood J. P., and Treiman A. H. 2014. The lunar apatite paradox. *Science* 344:400–402.

Bridges J. C., Catling D. C., Saxton J. M., Swindle T. D., Lyon I. C., and Grady M. M. 2001. Alteration assemblages in Martian meteorites: Implications for near-surface processes. *Space Science Reviews* 96:365–392.

Carroll M. R. and Webster J. D. 1994. Solubilities of sulfur, noble gases, nitrogen, chlorine, and fluorine in magmas. *Reviews in Mineralogy and Geochemistry* 30:231–279.

Chen Y., Liu Y., Guan Y., Eiler J. M., Ma C., Rossman G. R., and Taylor L. A. 2015. Evidence in Tissint for recent subsurface water on Mars. *Earth and Planetary Science Letters* 425:55–63.

Doherty A. L., Webster J. D., Goldoff B. A., and Piccoli P. M. 2014. Partitioning behavior of chlorine and fluorine in felsic melt–fluid (s)–apatite systems at 50 MPa and 850–950° C. *Chemical Geology* 384:94–111.

Filiberto J., Musselwhite D. S., Gross J., Burgess K., Le L., and Treiman A. H. 2010. Experimental petrology, crystallization history, and parental magma characteristics of olivine-phyric shergottite NWA 1068: Implications for the petrogenesis of "enriched" olivine-phyric shergottites. *Meteoritics & Planetary Science* 45:1258–1270.

Filiberto J., Treiman A. H., Giesting P. A., Goodrich C. A., and Gross J. 2014. High-temperature chlorine-rich fluid in the Martian crust: A precursor to habitability. *Earth and Planetary Science Letters* 401:110–115.

Goldoff B., Webster J. D., and Harlov D. E. 2012. Characterization of fluor-chlorapatites by electron probe microanalysis with a focus on time-dependent intensity variation of halogens. *American Mineralogist* 97:1103–1115.

Gross J., Filiberto J., and Bell A. S. 2013. Water in the Martian interior: Evidence for terrestrial MORB mantle-like volatile contents from hydroxyl-rich apatite in olivine–phyric shergottite NWA 6234. *Earth and Planetary Science Letters* 369:120–128.

Herd C. D. 2006. Insights into the redox history of the NWA 1068/1110 Martian basalt from mineral equilibria and vanadium oxybarometry. *American Mineralogist* 91:1616–1627.

Herd C. D., Borg L. E., Jones J. H., and Papike J. J. 2002. Oxygen fugacity and geochemical variations in the Martian basalts: Implications for Martian basalt petrogenesis and the oxidation state of the upper mantle of Mars. *Geochimica et Cosmochimica Acta* 66:2025–2036.

Howarth G. H., Pernet-Fisher J. F., Bodnar R. J., and Taylor L. A. 2015. Evidence for the exsolution of Cl-rich fluids in Martian magmas: Apatite petrogenesis in the enriched lherzolitic shergottite Northwest Africa 7755. *Geochimica et Cosmochimica Acta* 166:234–248.

Hu S., Lin Y., Zhang J., Hao J., Feng L., Xu L., Yang W., and Yang J. 2014. NanoSIMS analyses of apatite and melt inclusions in the GRV 020090 Martian meteorite: Hydrogen isotope evidence for recent past underground hydrothermal activity on Mars. *Geochimica et Cosmochimica Acta* 140:321–333.

Mathez E. A. 1984. Influence of degassing on oxidation states of basaltic magmas. *Nature* 310:371–375.

Mathez E. A. and Webster J. D. 2005. Partitioning behavior of chlorine and fluorine in the system apatite-silicate melt-fluid. *Geochimica et Cosmochimica Acta* 69:1275–1286.

McCubbin F. M., Elardo S. M., Shearer C. K., Smirnov A., Hauri E. H., and Draper D. S. 2013. A petrogenetic model for the comagmatic origin of chassignites and nakhlites: Inferences from chlorine-rich minerals, petrology, and geochemistry. *Meteoritics & Planetary Science* 48:819–853.

McCubbin F. M., Kaaden K. E. V., Tartèse R., Boyce J. W., Mikhail S., Whitson E. S., Bell A. S., Anand M., Franchi I. A., Wang J., and Hauri E. H. 2015. Experimental investigation of F, Cl, and OH partitioning between apatite and Fe-rich basaltic melt at 1.0–1.2 GPa and 950–1000 C. *American Mineralogist* 100:1790–1802.

McCubbin F. M., Boyce J. W., Srinivasan P., Santos A. R., Elardo S. M., Filiberto J., Steele A., and Shearer C. K. (Forthcoming). Heterogeneous distribution of H_2O in the Martian interior: Implications for the abundance of H_2O in depleted and enriched mantle sources. *Meteoritics & Planetary Science*. This issue, doi:10.1111/maps.12639.

Patiño Douce A. E. and Roden M. 2006. Apatite as a probe of halogen and water fugacities in the terrestrial planets. *Geochimica et Cosmochimica Acta* 70:3173–3196.

Peslier A. H., Hnatyshin D., Herd C. D. K., Walton E. L., Brandon A. D., Lapen T. J., and Shafer J. T. 2010. Crystallization, melt inclusion, and redox history of a Martian meteorite: Olivine-phyric shergottite Larkman Nunatak 06319. *Geochimica et Cosmochimica Acta* 74:4543–4576.

Sharp Z. D., Shearer C. K., McKeegan K. D., Barnes J. D., and Wang Y. Q. 2010. The chlorine isotope composition of the Moon and implications for an anhydrous mantle. *Science* 329:1050–1053.

Sharp Z. D., Shearer C. K., Agee C. B., and McKeegan K. D. 2011. The chlorine isotope composition of Mars (abstract #2534). 42nd Lunar and Planetary Science Conference. CD-ROM.

Sharp Z. D., Shearer C. K., Burger P. V., Agee C., and McKeegan K. 2014. The unique chlorine isotope composition of Mars: Implications for planetary formation and differentiation (abstract #1617). 45th Lunar and Planetary Science Conference. CD-ROM.

Shearer C. K., Sharp Z. D., McKeegan K. D., Burger P. V., McCubbin F. M., and Agee C. 2014. Chlorine isotopic composition of the Martian crust and mantle. Implications for their interactions, and magmatic processes. LPI Contribution 1791. Houston, Texas: Lunar and Planetary Institute. 1166 p.

Stormer J. C. Jr., Pierson M. L., and Tacker R. C. 1993. Variation of F and Cl X-ray intensity due to anisotropic diffusion in apatite. *American Mineralogist* 78:641–648.

Symes S. J., Borg L. E., Shearer C. K., and Irving A. J. 2008. The age of the Martian meteorite Northwest Africa 1195 and the differentiation history of the shergottites. *Geochimica et Cosmochimica Acta* 72:1696–1710.

Ustunisik G., Nekvasil H., and Lindsley D. 2011. Differential degassing of H2O, Cl, F, and S: Potential effects on lunar apatite. *American Mineralogist* 96:1650–1653.

Ustunisik G., Nekvasil H., Lindsley D. H., and McCubbin F. M. 2015. Degassing pathways of Cl-, F-, H-, and S-bearing magmas near the lunar surface: Implications for the composition and Cl isotopic values of lunar apatite. *American Mineralogist* 100:1717–1727.

Usui T., Alexander C. M. O'D., Wang J., Simon J. I., and Jones J. H. 2012. Origin of water and mantle–crust interactions on Mars inferred from hydrogen isotopes and volatile element abundances of olivine-hosted melt inclusions of primitive shergottites. *Earth and Planetary Science Letters* 357:119–129.

Webster J. D., Kinzler R. J., and Mathez E. A. 1999. Chloride and water solubility in basalt and andesite melts and implications for magmatic degassing. *Geochimica et Cosmochimica Acta* 63:729–738.

Williams J. T., Sharp Z. D., Shearer C. K., and Agee C. B. 2015. Confirmation of an isotopically light chlorine solar nebula and use of chlorine isotopes as a sensitive recorder of Martian crustal contamination (abstract #2641). 46th Lunar and Planetary Science Conference. CD-ROM.

Willmore C. C., Boudreau A. E., and Kruger F. J. 2000. The halogen geochemistry of the Bushveld Complex, Republic of South Africa: Implications for chalcophile element distribution in the lower and critical zones. *Journal of Petrology* 41:1517–1539.

SUPPORTING INFORMATION

Additional supporting information may be found in the online version of this article:

Data S1: Relative volatile fugacity calculations.